Int. J. Heat Mass Transfer. Vol. 36, No. 17, pp. 4141–4149, 1993
Printed in Great Britain

0017–9310/93 $6.00 + 0.00


# Analysis of radiation–natural convection interactions in 1-$g$ and low-$g$ environments using the discrete exchange factor method

M. KASSEMI
NASA Lewis Research Center, Cleveland, Ohio 44135, U.S.A.

and

M. H. N. NARAGHI
Mechanical Engineering Department, Manhattan College, Riverdale, New York 10471, U.S.A.

(*Received* 28 *August* 1992 *and in final form* 18 *May* 1993)

**Abstract**—A new numerical method is presented for the analysis of combined natural convection and radiation heat transfer with applications in many engineering situations such as materials processing, combustion and fire research. Because of the recent interest in the low gravity environment of space, attention is devoted to both 1-$g$ and low-$g$ applications. The two-dimensional mathematical model is represented by a set of coupled nonlinear integro–partial differential equations. Radiative exchange is formulated using the Discrete Exchange Factor method (DEF). This method considers point to point exchange and provides accurate results over a wide range of radiation parameters. Numerical results show that radiation significantly influences the flow and heat transfer in both low-$g$ and 1-$g$ applications. In the low-$g$ environment, convection is weak, and radiation can easily become the dominant heat transfer mode. It is also shown that volumetric heating by radiation gives rise to an intricate cell pattern in the top heated enclosure.

## INTRODUCTION

DUE TO its widespread application in various engineering disciplines, natural convective heat transfer in enclosures has received considerable attention in the past decade. It has been common practice to neglect the contribution of radiative heat transfer in most of the problems considered. Nevertheless, there are many engineering applications such as fire research, combustion, and material processing (specifically crystal growth and glass forming) where radiation can interact strongly with natural convection. Therefore, recently, some attention has also been devoted to the interaction between natural convection and radiation. It is now understood that under certain circumstances thermal radiation not only alters the temperature field, but due to the coupling between the energy and momentum transfer, it can also significantly modify the flow [1].

Most of the studies of the interaction between radiation and convection have focused on applications in 1-$g$ environment and the effect of the low-gravity environment on the interaction process has not yet been properly assessed. In ground-based applications, convective heat transfer often dominates radiation. But in the reduced acceleration environment of orbiting spacecraft, convection is weakened. In this case, radiation competing primarily with conduction, may predominate. One of the objectives of this paper is to show that due to the difference between the flow regimes which occur in 1-$g$ and low-$g$ applications, the effect of radiation heat transfer on convection can be quite different for the two cases.

A recent review by Ostrach [2] presents a comprehensive survey of natural convection in enclosures. It is evident, that as a result of the various analytical, experimental, and numerical studies of the past decade, the general characteristics of natural convective heat transfer are now known for various tilt angles, aspect ratios, Grashof and Prandtl numbers, and thermal boundary conditions. The interaction between radiation and natural convection has also been the subject of reviews by Viskanta [3] and Yang [1]. Early investigations of the interaction between convection and radiation for participating media have been carried out by Lauriat [4, 5] who used the P-1 differential approximation to represent radiative transfer in narrow vertical cavities. Later, Zhong *et al.* [6] extended the previous analyses by including the effects of tilt angle and variable properties; they employed a sliced exponential wide band scheme to represent radiation heat transfer. Finally, Yucel *et al.* [7] used the discrete ordinate method to study combined natural convection and radiation heat transfer from a scattering medium in a square cavity and Kassemi and Duval [8, 9] used a zonal approach to study the interaction of radiation with convection and its effect on crystal growth by vapor transport in rectangular enclosures.

A brief review of the above work indicates that

## NOMENCLATURE

| | |
|---|---|
| $A$ | surface area |
| $g$ | gravitational acceleration vector |
| $E$ | dimensionless emissive power |
| $Gr$ | Grashof number, $\beta g H^3 (T_h - T_c)/\nu^2$ |
| $H$ | height of the enclosure |
| $k_a$ | absorption coefficient |
| $k_s$ | scattering coefficient |
| $k_t$ | extinction coefficient, $k_a + k_s$ |
| $Nr$ | conduction–radiation number, $(\lambda(1-\gamma)/H)/\sigma T_h^3$ |
| $Nu_c$ | convective Nusselt number |
| $N_g$ | number of radiation nodes in the medium |
| $N_s$ | number of radiation nodes on the surfaces |
| $Pr$ | Prandtl number, $\nu/\alpha$ |
| $q''_w(\mathbf{r}_i)$ | dimensionless surface net radiative heat flux at $\mathbf{r}_i$ |
| $q'''(\mathbf{r}_i)$ | dimensionless volumetric net radiative heat source at $\mathbf{r}_i$ |
| $\mathbf{r}$ | position vector |
| $t$ | time |
| $T$ | temperature |
| $u$ | dimensionless velocity in the $x$-direction, $u^*/(\nu/H)$ |
| $v$ | dimensionless velocity in the $y$-direction, $v^*/(\nu/H)$ |
| $w$ | numerical integration weight factor |
| $x, y$ | dimensionless coordinates, $x^*/H$, $y^*/H$. |

Greek symbols

| | |
|---|---|
| $\alpha$ | thermal diffusivity |
| $\beta$ | coefficient of thermal expansion |
| $\gamma$ | temperature ratio, $T_c/T_h$ |
| $\varepsilon$ | emissivity |
| $\theta$ | dimensionless temperature, $T/T_h$ |
| $\lambda$ | thermal conductivity |
| $\nu$ | coefficient of dynamic viscosity |
| $\sigma$ | Stefan–Boltzmann constant |
| $\tau_0$ | optical thickness, $k_t \cdot H$ |
| $\phi$ | inclination angle |
| $\psi$ | dimensionless stream function, $\psi^*/\nu$ |
| $\omega$ | dimensionless vorticity, $\omega^*/(\nu/H^2)$ |
| $\omega_0$ | scattering albedo, $k_s/k_t$. |

Subscripts

| | |
|---|---|
| c | pertains to the cold wall |
| h | pertains to the hot wall |
| $i, j$ | denote receiving and sending nodes |
| s | denotes the enclosing wall surfaces |
| $w$, 1, 2 | denote the sidewalls. |

Superscript

| | |
|---|---|
| * | denotes dimensional quantity. |

Radiation exchange factors

| | |
|---|---|
| $\overline{DVV}(\mathbf{r}_i, \mathbf{r}_j)$ | total exchange factor between volumes |
| $\overline{DVS}(\mathbf{r}_i, \mathbf{r}_j)$ | total exchange factor between volume and surface |
| $\overline{DSV}(\mathbf{r}_i, \mathbf{r}_j)$ | total exchange factor between surface and volume |
| $\overline{DSS}(\mathbf{r}_i, \mathbf{r}_j)$ | total exchange factor between surfaces. |

because of the complexity of the nonlinear integro–partial differential equations which describe this class of problems, researchers have usually been forced to invoke approximate techniques to represent multidimensional radiation exchange. The P-1 differential approximation has served as a favorite radiation model [4, 5]. This is mainly because the differential approximation reduces the integral equations describing radiative transfer into a set of differential equations which are compatible with the equations for transport of heat and momentum. The P-1 approximation is, however, severely limited and strictly speaking, the method is only accurate for optically thick media. The discrete ordinate method [7] has proved to be more accurate. This method works well for a highly scattering medium. Unfortunately, it suffers from the so-called ray effects and its accuracy deteriorates as the level of scattering in the medium decreases [10, 11].

One of the promising techniques for the computation of multidimensional radiative exchange is the Discrete Exchange Factor (DEF) method which was applied to pure radiation heat transfer in a rectangular enclosure by Naraghi and Kassemi [12]. Unlike the differential approximation, the DEF method provides an *exact* treatment of multidimensional radiative transfer over a wide range of optical thicknesses. In contrast to the discrete ordinate method, it provides accurate results for both non-scattering and highly scattering media [12].

The main advantage of DEF over the zone method is that it considers point to point radiation exchange. Therefore, for a two-dimensional problem, only one numerical integration is needed to evaluate the node-to-node exchange factors. In contrast, the zone method is based on zone to zone exchange. Thus, for a two-dimensional problem, five integrations are necessary to evaluate the zone-to-zone direct exchange areas. The other advantage of the DEF method is that it can accommodate a variety of different integration schemes and nodal arrangements. These range from the Gaussian quadratures which provide the best accuracy, through Simpson and trapezoidal methods which can easily match the uniform and nonuniform

nodal distributions of the finite difference grids, to the rectangular scheme which is ideally suited for incorporation into the finite element codes [13]. Therefore, the method is very versatile. The second objective of this paper is to demonstrate the effective incorporation of the DEF method into finite-difference codes for combined heat transfer.

## MATHEMATICAL FORMULATION

Consider a square cavity of height $H$, as depicted in Fig. 1. The cavity is at an angle $\phi$ with respect to the gravitational vector. As in the classical natural convection problem, a hot wall, at a uniform temperature $T_h$, forms one side of the enclosure, while a cold wall, at a uniform temperature $T_c$, forms the other. The sidewall boundaries are either insulated or subject to an imposed temperature profile. The boundary surfaces are assumed to be diffuse and gray with emissivity $\varepsilon$. The fluid is modeled as a gray isotropically scattering medium with albedo $\omega_0$.

Transport in the cavity is governed by a system of nonlinear coupled conservation equations for mass, momentum, and energy. Radiative transfer is represented by integro–differential equations. Using the stream-function vorticity formulation and invoking the Boussinesq approximation, the momentum equation is cast into the following dimensionless form:

$$u\frac{\partial\omega}{\partial x}+v\frac{\partial\omega}{\partial y}=\frac{\partial^2\omega}{\partial x^2}+\frac{\partial^2\omega}{\partial y^2}+\frac{Gr}{1-\gamma}\left(\frac{\partial\theta}{\partial x}\sin\phi+\frac{\partial\theta}{\partial y}\cos\phi\right) \quad (1)$$

where

$$u=\frac{\partial\psi}{\partial y} \quad v=-\frac{\partial\psi}{\partial x} \quad (2)$$

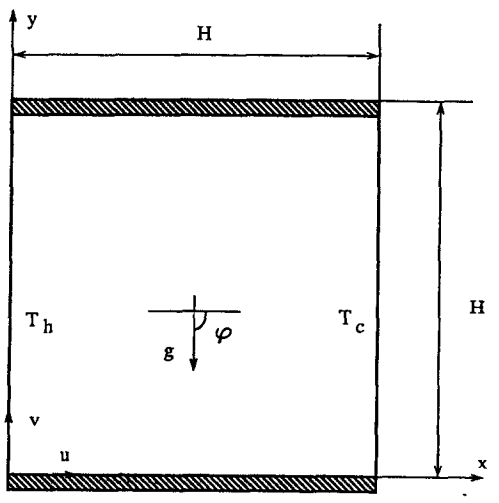


FIG. 1. The square enclosure.

and

$$\frac{\partial^2\psi}{\partial x^2}+\frac{\partial^2\psi}{\partial y^2}=-\omega. \quad (3)$$

This equation is subject to the non-slip boundary conditions:

$$u=v=0 \quad \text{for} \quad y=0,1 \quad 0\leqslant x\leqslant 1 \quad (4)$$

$$u=v=0 \quad \text{for} \quad x=0,1 \quad 0\leqslant y\leqslant 1. \quad (5)$$

The energy equation is written as a balance between convection, conduction and radiation. In dimensionless form, it is given by:

$$u\frac{\partial\theta}{\partial x}+v\frac{\partial\theta}{\partial y}=\frac{1}{Pr}\left\{\left(\frac{\partial^2\theta}{\partial x^2}+\frac{\partial^2\theta}{\partial y^2}\right)-\frac{\tau_0}{Nr}(q_r''')\right\}. \quad (6)$$

The boundary conditions for the energy equation are

$$\theta=\theta_h,\theta_c \quad \text{for} \quad x=0,1 \quad 0\leqslant y\leqslant 1 \quad (7)$$

$$\theta=\theta_1,\theta_2 \quad \text{for} \quad y=0,1 \quad 0\leqslant x\leqslant 1 \quad (8)$$

where temperatures $\theta_h=1$, $\theta_c=\gamma$ and $\theta_1$ and $\theta_2$ are defined below.

The radiation source term in the energy equation is represented by the net radiative heat flux. Using the continuous exchange factor notation, this quantity is written as:

$$q_r'''(\mathbf{r}_i)=4(1-\omega_0)\theta^4(\mathbf{r}_i)-\int_S \varepsilon\theta^4(\mathbf{r}_j)\overline{DSV}(\mathbf{r}_j,\mathbf{r}_i)-\int_V 4(1-\omega_0)\theta^4(\mathbf{r}_j)\overline{DVV}(\mathbf{r}_j,\mathbf{r}_i). \quad (9)$$

In the above equation $\overline{DSV}$ and $\overline{DVV}$ are respectively the surface-to-volume and volume-to-volume total exchange factors. They represent the fraction of energy emitted from a differential surface or volume at $\mathbf{r}_j$ that reaches a differential surface or volume at $\mathbf{r}_i$, directly, or after multiple reflections at the walls and/or scattering in the medium. For details, the reader is referred to Naraghi and Kassemi [12].

Thermal boundary conditions are very important in combined heat transfer. If the sidewall temperatures are fixed, then temperatures $\theta_1$ and $\theta_2$ are prescribed parameters. For example, they may be given by the following linear profile:

$$\theta_w=\theta(x,0)=\theta(x,1)=1-x \quad \text{for} \quad w=1,2. \quad (10)$$

On the other hand, if we consider the sidewalls to be insulated, then the wall temperatures are unknown variables of the problem. They have to be determined as part of the overall solution through a balance between radiation and convection (conduction) at the insulted walls. That is:

$$\nabla\theta\cdot\hat{n}_w=\left(\frac{1}{Nr}\right)q_w'' \quad \text{for} \quad w=1,2. \quad (11)$$

Here, $q_w''$ represents the net radiative heat flux at the

wall and is described by the following integral equation.

$$q''_w(\mathbf{r}_i) = \varepsilon\theta^4(\mathbf{r}_i) - \int_S \varepsilon\theta^4(\mathbf{r}_j)\overline{DSS}(\mathbf{r}_j, \mathbf{r}_i) - \int_V 4(1-\omega_0)\theta^4(\mathbf{r}_j)\overline{DVS}(\mathbf{r}_j, \mathbf{r}_i). \quad (12)$$

In the preceding equation, $\overline{DSS}$ and $\overline{DVS}$ are respectively the surface-to-surface and volume-to-surface total exchange factors between the sending location, $\mathbf{r}_j$, and receiving location, $\mathbf{r}_i$. Again, these expressions include the effect of multiple reflection and scattering, as well as, direct exchange between the surfaces and volumes [12].

## NUMERICAL FORMULATION

In order to solve the system of nonlinear coupled partial differential equations, a staggered grid was utilized. In a staggered mesh, any four adjacent stream function nodes form the four corners of a control volume cell. At the center of this cell, the vorticity and temperature nodes are specified. The momentum and energy equations are discretized by the nominally third order accurate QUICK scheme [14]. The vorticity boundary conditions are determined in a manner consistent with the overall accuracy of the method [14]. In the limiting case of natural convection in a square enclosure, current results for velocity, stream function, temperature, and Nusselt number (for $20 \times 20$ and $40 \times 40$ grids) were compared with benchmark solutions provided by de Vahl Davis [15] and agreement was found to be excellent.

The radiation source terms are lagged one step behind the flow calculations. The source term in any control volume is simply calculated as an average of the net radiative fluxes at the corner stream function nodes which are evaluated according to DEF (equations (9) and (12)) as:

$$q''_{w_i} = E_{w_i} - \sum_{j=1}^{N_s} w_{s_j} E_{s_j} \overline{DS_j S_i} - \sum_{j=1}^{N_g} w_j E_j \overline{DV_j S_i} \quad (13)$$

and

$$q'''_i = E_i - \sum_{j=1}^{N_s} w_{s_j} E_{s_j} \overline{DS_j V_i} - \sum_{j=1}^{N_g} w_j E_j \overline{DV_j V_i}. \quad (14)$$

The dimensionless surface and volume emissive powers can be expressed in terms of temperature via $E_{w_j} = \varepsilon_j \theta^4_{w_j}$ and $E_j = 4(1-\omega_0)\theta^4_j$, respectively.

In this formulation, radiative heat transfer is represented in terms of exchange between surface and volume nodes. The index $i$, pertains to a receiving surface or volume node and the index, $j$, denotes the sending surface or volume node. The weight factors, $w_s$ and $w$, correspond to the numerical integration scheme employed. As mentioned before, DEF can accommodate a variety of different integration schemes. Naturally, the distribution of the nodes, $i$ and $j$, and the magnitude of the weights, $w_s$ and $w$, depend on the particular integration scheme employed. Experience has shown that the Gaussian quadrature integration scheme produces the most accurate results. Unfortunately, when using this method, the integration points, which are the zeros of the interpolating polynomial (i.e. Legendre, Chebyshev, etc.), do not usually coincide with the grids in the finite difference formulations. On the other hand, the trapezoidal, Simpson's and rectangular methods, while lower in accuracy, can easily accommodate the finite difference grid structures. Hence, they provide greater flexibility. In any case, because in a combined heat transfer situation, the grid size is determined by the discretization of the flow equations, the number of nodes is usually more than adequate for all the four schemes to provide accurate radiation predictions.

In this work, Simpson's integration scheme was chosen as a viable compromise between accuracy and flexibility. In the parametric range of interest, the details of the flow were adequately resolved by a $20 \times 20$ grid. The integrity of the DEF method was verified through comparison with the limiting solutions provided by Larsen [16] for combined conduction and radiation in square enclosures. The agreement between the temperature and wall heat flux results was within 1%, for the $11 \times 11$ grid used by Larsen.

## RESULTS AND DISCUSSION

The results presented here are limited to two basic configurations: *horizontal*, with the gravity vector perpendicular to the imposed temperature gradient, and *vertical*, with the gravity vector parallel to the imposed temperature gradient. Since, only the general characteristics of radiation–convection interactions are of interest, it is assumed that $Pr = 0.70$, $\varepsilon = 1.0$, and $\omega_0 = 0.0$.

The enclosure with insulated side walls at 1-$g$ is considered first. In the absence of radiation, the flow and temperature profiles are shown in Fig. 2. In this orientation ($\phi = 90^\circ$), the imposed temperature difference is perpendicular to the gravitational vector. Therefore, at a $Gr = 1 \times 10^5$, a strong recirculating flow ensues in the cavity. The velocity vector field and stream function plot presented in Fig. 2 indicate the formation of two co-rotating vortices near the center of the enclosure. From the temperature contours, it is apparent that thermal boundary layers form along the hot and cold walls. The flow in the enclosure is driven mainly by the steep temperature gradients in these boundary layers. Therefore, as will be seen later, this flow is very sensitive to the thermal conditions in the vicinity of the hot and cold walls which can be easily perturbed by radiation. The temperature profiles of the insulated walls are shown in Fig. 3. Note that

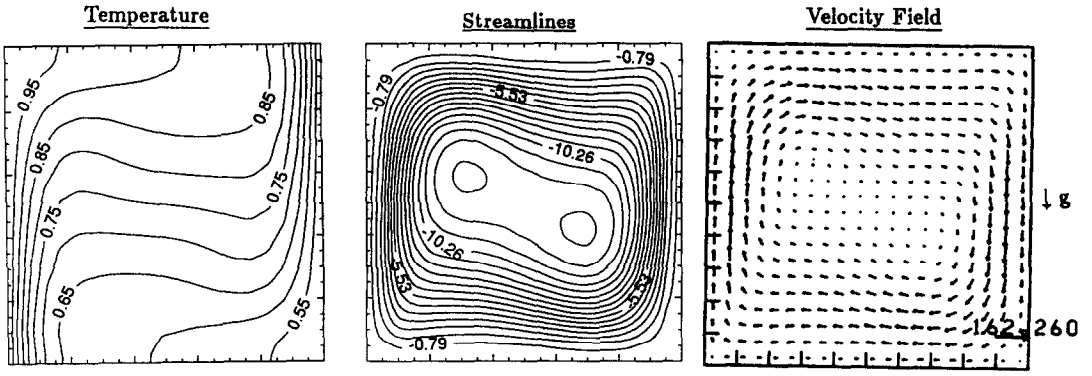


FIG. 2. Flow inside the enclosure in absence of radiation effects; $Gr = 1 \times 10^5$, $\gamma = 0.50$, $Nr \to \infty$, $\tau_0 = 0.0$.

because of the strong recirculating flow, there is a considerable difference between the temperature of the convectively cooled bottom wall, and the convectively heated top wall.

The effects of radiation heat transfer are presented in Figs. 4–6 for $Nr = 0.10$. The transparent medium ($\tau_0 = 0.0$) is considered first. In this case, the vapor does not participate in the radiative transfer process, and radiation exchange only takes place between the enclosing surfaces. Figure 4 shows that, as a result of radiation exchange among the insulated walls and the hot wall, the temperature of the bottom wall drastically increases. The bottom wall, in turn, heats the vapor flowing above it, especially close to the hot wall. Consequently, as shown in Fig. 5, the axial temperature gradients near the hot wall are weakened and the thermal boundary layer near the hot wall thickens. The velocity and stream function plots of Fig. 5 indicate that the central vortices become weaker. Note, however, that the flow near the cold wall remains strong in order to dissipate the heat added by radiation into the cold sink.

The participation of the medium in the combined heat transfer process is considered next. The results for an optical thickness of 1.0 are presented in Fig. 6. In this case, the medium can absorb radiation directly. Therefore, the fluid near the hot wall is affected by radiation heat transfer in two ways. First, it is heated directly by absorbing the radiation emitted by the hot wall. Secondly, it is affected indirectly by the radiative heat which is absorbed by the bottom wall and then convected into the medium. As indicated by the temperature contours in Fig. 6, this injection of heat by radiation completely disrupts the thermal boundary layer near the hot wall. Flow near the cold wall, however, becomes slightly stronger to dissipate the extra heat delivered by radiation into the cold sink. Therefore, the double-vortex flow of the no-radiation case (Fig. 2) is replaced by the very vigorous single-cell recirculating flow shown in Fig. 6.

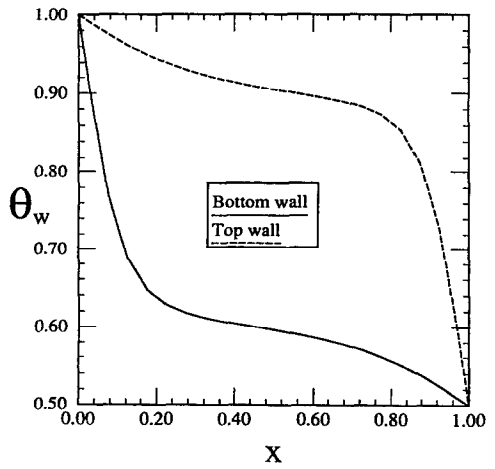


FIG. 3. Wall temperature distribution in the absence of radiation effects; $Gr = 1 \times 10^5$, $\gamma = 0.50$, $Nr \to \infty$, $\tau_0 = 0.0$.

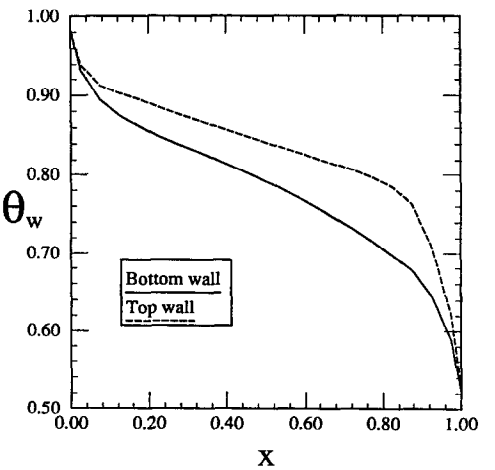


FIG. 4. Wall temperature distribution in the presence of surface radiation exchange; $Gr = 1 \times 10^5$, $\gamma = 0.50$, $Nr = 0.10$, $\tau_0 = 0.0$.

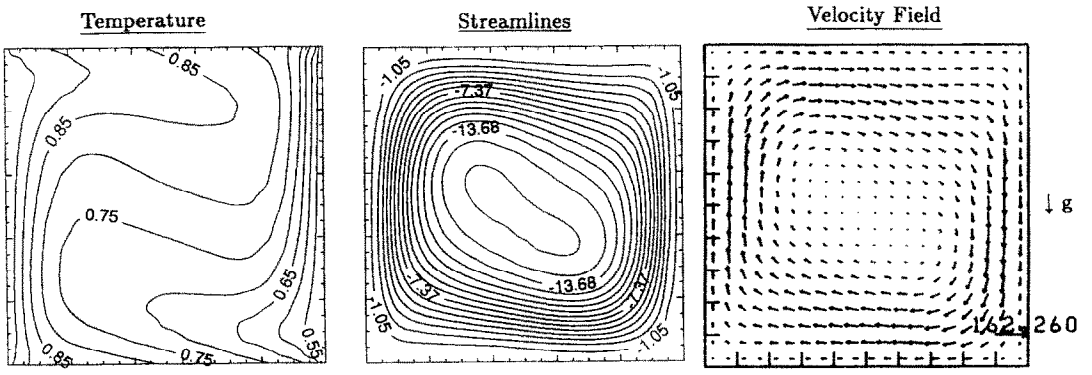


FIG. 5. Interaction of radiation with convection for a transparent medium; $Gr = 1 \times 10^5$, $\gamma = 0.50$, $Nr = 0.10$, $\tau_0 = 0.0$.

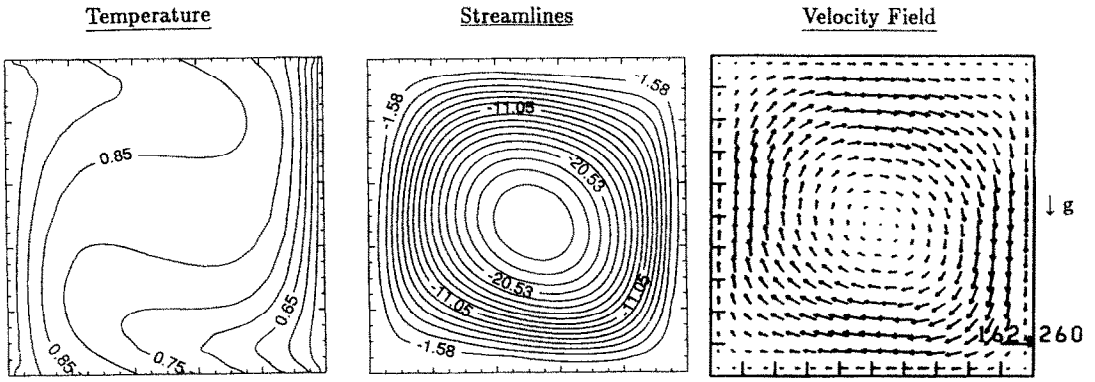


FIG. 6. Interaction of radiation with convection for a participating medium; $Gr = 1 \times 10^5$, $\gamma = 0.50$, $Nr = 0.10$, $\tau_0 = 1.0$.

In order to summarize the effects of radiation on the boundary-layer driven flow and heat transfer which prevail in 1-$g$ applications, the behavior of the convective Nusselt number (Table 1) is considered. Both surface and volumetric radiation exchange cause a significant augmentation of the convective heat transfer at the cold wall. This is due to the fact that the extra heat imparted to the fluid by radiation has to be convected into the cold sink. Table 1, however, indicates that because of radiative interactions, the convective Nusselt number in the hot wall decreases. This is because both volumetric and surface radiation exchange contribute to the disintegration of the thermal boundary layer near the hot wall.

Next, attention is focused on the situation which may occur at a $g$-level of $(1 \times 10^{-3})g$, where convection is weakened considerably. Therefore, radiation has to compete only with conduction for the control of heat transfer.

Table 1. Effect of radiation on the mean convective Nusselt number

| | $Gr = 1 \times 10^5$ | | $Gr = 700$ | |
|---|---|---|---|---|
| Case | $Nu_{cc}$ | $Nu_{ch}$ | $Nu_{cc}$ | $Nu_{ch}$ |
| $Nr = \infty$, $\tau_0 = 0.0$ | 4.152 | 4.152 | 1.033 | 1.033 |
| $Nr = 0.10$, $\tau_0 = 0.0$ | 4.750 | 3.381 | 2.407 | 1.480 |
| $Nr = 0.10$, $\tau_0 = 1.0$ | 5.295 | 2.915 | 3.371 | 1.832 |

The low-$g$ case in the absence of radiation effects is considered first. This is presented in Fig. 7 for $Gr = 700$. Note that in this case, the driving force for the flow is considerably reduced. Therefore, the recirculating flow is much weaker than the previous high $Gr$ case and it can deform the temperature contours only slightly. Here, conduction is the mode of heat transfer. Unlike the previous boundary layer driven flow, this recirculating flow is driven by the temperature gradients in the core. As shown in Fig. 8, the temperatures of the insulated walls are almost linear. The top wall is at a slightly higher temperature because it is heated by the hot fluid flowing in the top portion of the cavity.

The effects of surface radiation exchange are studied for a transparent fluid in the enclosure. It is evident from Fig. 9 that, as a result of radiation emitted by the hot wall and absorbed by the insulated walls, the temperature of the sidewalls are drastically changed. Because of radiation exchange between the insulated walls, their temperature profiles become almost ident-

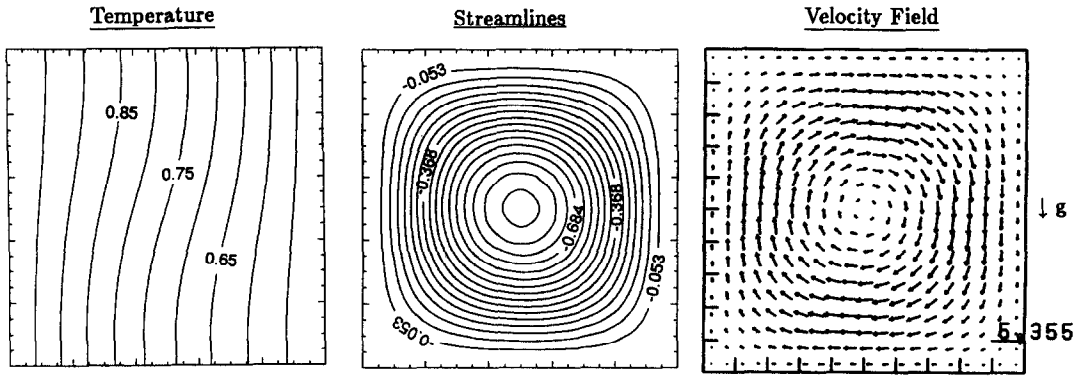


FIG. 7. Flow inside the enclosure in absence of radiation effects; $Gr = 700$, $\gamma = 0.50$, $Nr \to \infty$, $\tau_0 = 0.0$.

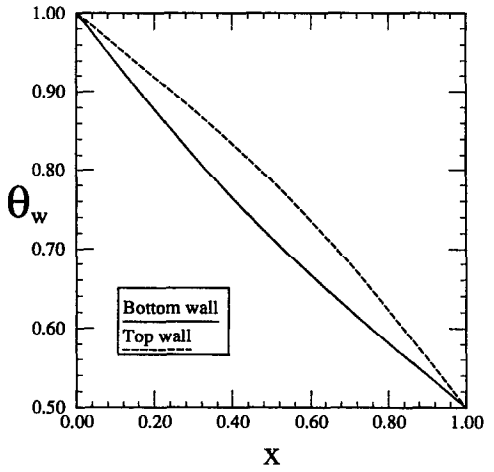


FIG. 8. Wall temperature distribution in the absence of radiation effects; $Gr = 700$, $\gamma = 0.50$, $Nr \to \infty$, $\tau_0 = 0.0$.

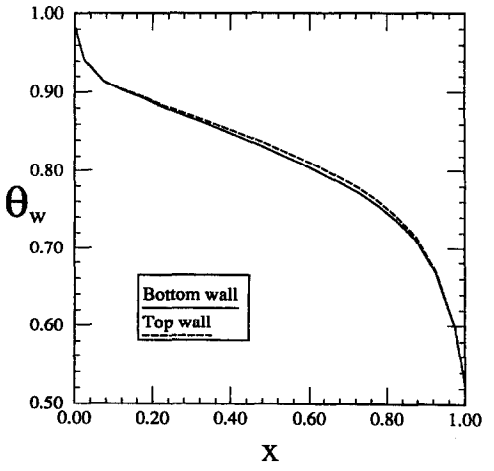


FIG. 9. Wall temperature distribution in the presence of surface radiation exchange; $Gr = 700$, $\gamma = 0.50$, $Nr = 0.10$, $\tau_0 = 0.0$.

ical. The temperature contours in Fig. 10 indicate that the insulated walls impart the heat delivered by radiation to the recirculating fluid. This heat has to be dissipated at the cold wall. Steep axial temperature gradients are set up near the cold wall to conduct this extra heat into the sink. Consequently, as shown in the stream function and velocity field plots, the center of the recirculating cell moves slightly toward the cold wall.

In low-$g$ applications, the participation of the fluid in radiative transfer affects the temperature contours significantly. The results presented in Fig. 11 are for $\tau_0 = 1.0$ and $Nr = 0.10$. In this case, because the medium absorbs the radiation emitted by the hot source, less radiation reaches the insulated walls. Hence, the transverse temperature gradients at these walls are reduced in comparison to those for the transparent fluid (see Fig. 10). Because the flow is weak, radiation becomes the dominant heat transfer mode in the medium; as a result of the distributive nature of the emission–absorption process, fluid temperatures in the transverse direction become very uniform. However, the axial temperature gradients must remain high, especially near the cold wall, in order to dissipate the extra heat added by radiation into the cold sink. Therefore, flow near the cold wall is intense and the center of the recirculating cell moves further towards this wall.

The effect of radiation on convective heat transfer in the low $Gr$ regime is again summarized in Table 1. It is evident that because of radiation, convective heat transfer at the cold wall increases significantly. The convective Nusselt number at the hot wall also increases in the presence of radiation. This is in contrast to the behavior noted for the high $Gr$ flow and is mainly due to the drop in the insulated wall temperatures near the hot wall caused by radiative exchange (see Figs. 8 and 9). In this case, the fluid near the hot wall receives less heat from the sidewalls and, therefore, it can draw more heat by conduction from the hot wall.

Finally, the square cavity, in a top heating configuration ($\phi = 0$) is considered under 1-$g$ conditions. This orientation is often used to eliminate convection

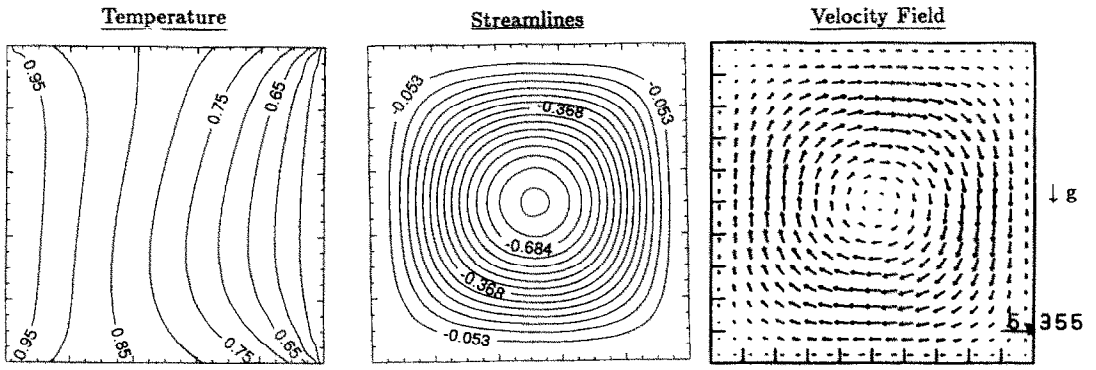


FIG. 10. Interaction of radiation with convection for a transparent medium; $Gr = 700$, $\gamma = 0.50$, $Nr = 0.10$, $\tau_0 = 0.0$.

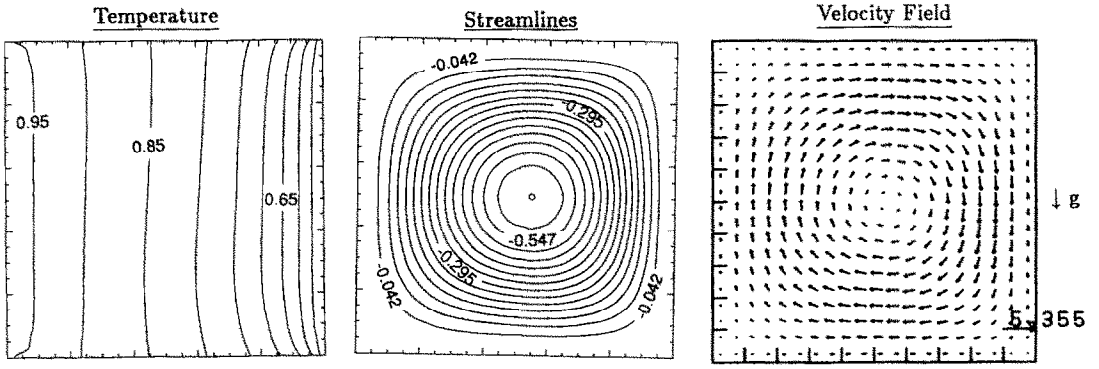


FIG. 11. Interaction of radiation with convection for a participating medium; $Gr = 700$, $\gamma = 0.50$, $Nr = 0.10$, $\tau_0 = 1.0$.

on earth. However, the results presented in Fig. 12 show that the convective stability of the top heated enclosure is disrupted by radiation heat transfer. In this case, linear temperature profiles are imposed on the sidewalls as described by equation (10); thus the

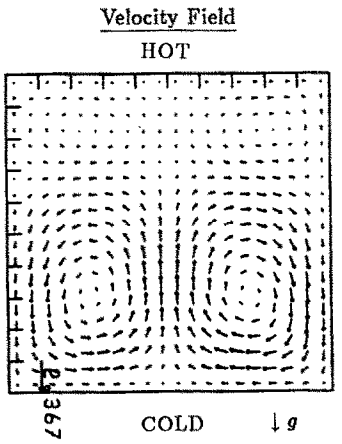


FIG. 12. Radiation-induced convection in the top heated square cavity subject to prescribed linear wall temperature profiles; $Gr = 1 \times 10^4$, $\gamma = 0.80$, $Nr = 0.01$, $\tau_0 = 1.0$.

effects of surface radiation exchange are absent. At a moderate optical thickness of 1.0, radiation emanating from the walls penetrates into the medium. The fluid in the midsection of the cavity has a better view of the hot sources than the fluid near the sidewalls. Therefore, it is heated more by radiation and rises until it loses momentum. As a result of this motion induced by radiation, two vortices develop near the cold wall which drive two weaker counter-rotating vortices near the top of the enclosure.

## CONCLUSIONS

The interaction between thermal radiation and natural convection in a square enclosure was studied numerically. The Discrete Exchange Factor (DEF) method proved to be convenient, versatile, and accurate for calculating radiation exchange in combined heat transfer problems. Radiation was found to wield a significant influence in both low-$g$ and 1-$g$ applications:

- In the high $Gr$ situations which dominate most ground-based applications, because of both surface and volumetric radiation exchange, the boundary

layer driven flow is disrupted and the flow structure is considerably altered.

- In the low $Gr$ flows, which often prevail in low-$g$ environment, the temperature distribution in the enclosure is significantly affected by radiation. In this situation, radiation has to compete solely with conduction. Therefore, it becomes the dominant heat transfer mode even for moderate $Nr$ and $\tau_0$ values and has two major effects:

1. it makes the temperature in the medium very uniform;
2. it modifies the behavior and the magnitude of convective heat transfer at the cold sink.

- Finally, numerical predictions show that local temperature gradients induced by radiation heat transfer disrupts the convective stability of the top-heated enclosure in the 1-$g$ environment.

*Acknowledgement*—The support of Microgravity Science and Applications Division at National Aeronautics and Space Administration and the valuable system-related assistance of Ron Gaug and Dave Thompson of the Computational Materials Laboratory at Lewis Research Center is gratefully acknowledged.

## REFERENCES

1. K. T. Yang, Numerical modeling of natural convection–radiation interactions in enclosures. In *Heat Transfer 1986*, pp. 131–140. Hemisphere, Washington D.C. (1986).
2. S. Ostrach, Natural convection in enclosures, *J. Heat Transfer* **110,** 1175–1195 (1988).
3. R. Viskanta, Radiation heat transfer, *Fortschritte Der Verfahrenstechnik* **22,** 51–81 (1984).
4. G. Lauriat, Combined radiation–convection in gray fluids enclosed in vertical cavities, *ASME J. Heat Transfer* **104,** 609–615 (1982).
5. G. Lauriat, Numerical study of the interaction of natural convection with radiation in nongray gases in a narrow vertical cavity. In *Heat Transfer 1982*, pp. 153–158. Hemisphere, Washington D.C. (1982).
6. Z. Y. Zhong, K. T. Yang and J. R. Lloyd, Variable-property natural convection in tilted enclosures with thermal radiation, *Numerical Methods in Heat Transfer* (Edited by R. W. Lewis), Vol. 3, pp. 209–218 (1985).
7. A. Yucel, S. Acharya and M. L. Williams, Combined natural convection and radiation in a square enclosure, *Proceedings of the 1988 National Heat Transfer Conference* (Edited by H. R. Jacobs), HTD-96, pp. 209–218 (1988).
8. M. Kassemi and W. M. B. Duval, Interaction of surface radiation with convection in crystal growth by vapor transport, *J. Thermophys. Heat Transfer* **11,** 454–461 (1990).
9. M. Kassemi and W. M. B. Duval, Effect of gas and surface radiation on crystal growth from the vapor phase, *J. PhysicoChemical Hydrodynamics* **11,** 737–751 (1989).
10. W. A. Fiveland, Discrete-ordinate solution of the radiative transport equation for rectangular enclosures, *J. Heat Transfer* **106,** 699–706 (1984).
11. J. J. Duderstadt and W. R. Martin, *Transport Theory*. Wiley, New York (1979).
12. M. H. N. Naraghi and M. Kassemi, Analysis of radiative transfer in rectangular enclosures using a discrete exchange factor method, *ASME J. Heat Transfer* **111,** 1117–1120 (1989).
13. C. Saltiel and M. H. N. Naraghi, Analysis of radiative heat transfer in participating media using arbitrary nodal distribution, *Numer. Heat Transfer. Part B* **17,** 227–243 (1990).
14. B. P. Leonard, A convectively stable, third order finite difference method for steady two-dimensional flow and heat transfer. In *Numerical Properties and Methodologies in Heat Transfer* (Edited by T. M. Shih), pp. 211–226. Hemisphere, Washington D.C. (1983).
15. G. de Vahl Davis, Natural convection of air in a square cavity: a bench mark numerical solution, *Int. J. Numer. Methods Fluids* **3,** 249–264 (1983).
16. M. E. Larsen, The exchange factor method: an alternative zonal formulation for analysis of radiating enclosures containing participating media, Ph.D. Dissertation, The University of Texas, Austin, Texas (1983).